15 Acoustic Daylight Imaging in the Ocean

Michael J. Buckingham

Scripps Institution of Oceanography, La Jolla, CA, USA

15.1 Introduction

Seawater is essentially transparent to sound and opaque to all other forms of radiation, including light. Acoustic techniques are thus a preferred choice for probing the ocean depths. Two types of acoustic systems, passive sonar and active sonar, are commonly used as detection devices in the ocean [1]. A passive sonar simply listens for the sound radiated by a target such as a submarine, whereas an active sonar transmits an acoustic pulse and listens for returning echoes from objects of interest. Apart from their military applications, active sonars are used in various configurations for numerous purposes, from simple echo sounding to mapping the seafloor.

Besides the signals of interest, both passive and active sonars respond to ambient noise in the ocean, which tends to degrade the performance of such systems. The noise is generated partly by natural sources including wave breaking [2], precipitation [3], and, of course, a variety of biological organisms ranging from marine mammals [4, 5, 6, 7] to snapping shrimp [8, 9] and croakers [10]; and also by anthropogenic sources, notably surface shipping, and offshore exploration and drilling for hydrocarbons. Considerable effort has been devoted to suppressing the effects of the noise on active and passive sonars, with a view to enhancing the signal-to-noise ratio at the output of the system.

Handbook of Computer Vision and Applications
Volume 1
Sensors and Imaging

ISBN 0-12-379771-3/$30.00

Acoustic noise propagates through the ocean in much the same way that light propagates through the atmosphere, and in so doing acquires information about objects it encounters in its path. This suggests that an alternative to noise suppression is noise exploitation, in which information, in the form of an image of the environment, is obtained from the ensonification provided by the noise field. A reasonable optical analog is conventional photography in the atmosphere using daylight as the illumination; a photographic image of an object can be obtained, even though the object itself radiates no light and no artificial source of light, such as a photoflood or flashgun, is employed to illuminate the scene. Evidently, photography with daylight is neither "passive" nor "active," but instead relies on the ambient light scattered from the object space to create the image.

Beneath the sea surface the *ambient noise* field provides a form of "acoustic daylight." The noise is a stochastic radiation field with energy traveling in all directions, and as such has much in common with the diffuse ambient light field filtering through a cloud layer. This suggests that the noise has the potential for *acoustic imaging*, although the highest usable frequency is expected to be around 100 kHz. (At higher frequencies the propagating noise is likely to be masked by the localized thermal noise [11, 12] of the water molecules, which carries no imaging information.) The wavelength of sound in seawater at a frequency of 100 kHz is 1.5 cm, which is orders of magnitude greater than optical wavelengths, implying that the resolution of the images obtained from the ambient noise field will not match that of the pictures from a photographic camera.

The first issue to address, however, is not the quality of acoustic daylight images but whether such images can be formed at all. In this chapter, some early experiments on scattering of ambient noise from targets on the seabed are briefly discussed, the first acoustic daylight imaging system is described, and some results from deployments of the system in the ocean off southern California are presented. These images clearly demonstrate that, in certain ambient noise environments, it is possible to create stable, recognizable acoustic daylight images of targets at ranges out to 40 m.

15.2 The pilot experiment

In 1991, a simple experiment [13] was conducted off Scripps pier, southern California, where the nominal water depth is 7 m. The experiment was designed to determine whether ambient noise scattered by an object in the ocean is detectable using a low-noise, directional acoustic receiver. The targets were three rectangular ($0.9 \times 0.77\,\mathrm{m}^2$) wooden panels faced with closed-cell neoprene foam, which, being loaded with

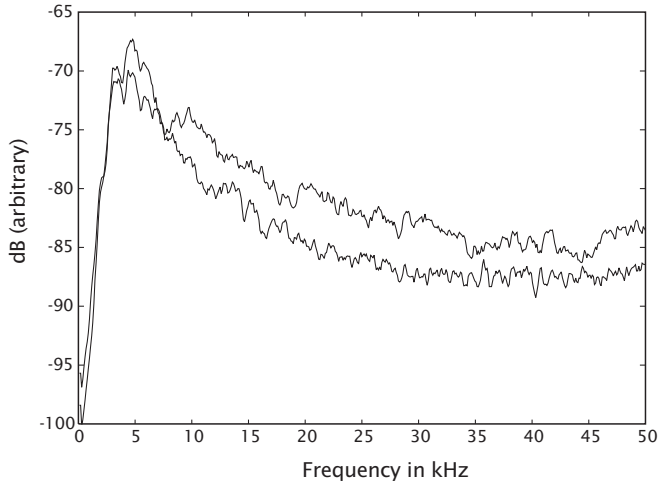

Figure 15.1: *Noise spectra obtained in the pilot experiment with the targets "on" (upper trace) and "off" (lower trace).*

air, is an efficient acoustic reflector. A single hydrophone mounted at the focus of a parabolic reflector of diameter 1.22 m was used as the directional acoustic receiver. The frequency response of the system extended from 5 to 50 kHz, and at the highest frequency the beamwidth was $\approx 3.6^{\circ}$.

Divers deployed the targets and the receiver on the seabed, separated by a horizontal distance of 7 m. The target panels were placed vertically and could be rotated about a vertical axis, allowing them to be oriented either normal to or parallel to the line of sight, the "on" and "off" positions, respectively. In the "on" configuration, the three target panels formed, in effect, a single rectangular target of height 0.9 m and width 2.5 m. At a frequency of 9 kHz, the angular width of the main lobe of the receiver, as measured at the −6 dB points, matched the angle subtended by this extended target, and hence at higher frequencies the angular width of the target was greater than that of the beam.

Ambient noise data were collected sequentially with the target panels in the "on" and "off" positions. Typically, it took 15 to 30 min for the divers to rotate the panels from one configuration to the other. Figure 15.1 shows an example of the noise spectra that were obtained in the experiment. Over the frequency band of interest, it can be seen that the spectral level is higher by some 3 dB with the panels in the "on" position, a result that was found consistently throughout the experiment. The excess noise level observed with the panels "on" suggests that the noise originated behind the receiver, a situation analogous to taking a photograph with the sun behind the camera. In fact, a subsequent ex-

periment [14] established that the dominant noise sources were snapping shrimp located around the pilings of the pier, which was indeed immediately behind the acoustic receiver.

With most of the noise sources located behind the receiver, little if any noise radiation was blocked by the target but a significant portion was scattered back towards the dish. Evidently, the presence of the panels modified the observed noise intensity significantly. Such behavior is potentially important, as it provides the basis for incoherent imaging with ambient noise. In effect, what had been achieved with the single-beam receiver was just one pixel of an image. Based on this result from the pilot experiment, it seemed possible that, by increasing the number of beams and mapping the noise intensity in each into a pixel on a computer monitor, a visually recognizable image of the target space could be achieved. The objective of the next stage of the acoustic daylight imaging project [15] was to design and build a multibeam, broadband acoustic receiver with the capability of resolving meter-sized objects at ranges of about 50 m.

15.3 ADONIS

In designing the multibeam acoustic receiver, it was decided that a minimum of about 100 pixels would be needed to produce an acoustic daylight image. The question then arose as to what type of detector should be used for the purpose? A possible design solution to the problem would have been a phased array with an aperture in the region of 3 m. This approach, however, was not pursued for several practical reasons, one of which was the heavy computational load imposed by the beamforming. Instead, a reflector technology was again employed, this time in the form of the *Acoustic Daylight Ocean Noise Imaging System* (ADONIS). The design of ADONIS is very much more complex than the parabolic system used in the pilot acoustic daylight experiment. Before it was constructed, the imaging performance of ADONIS was simulated using a numerical algorithm based on the Helmholtz-Kirchhoff scattering integral [16]; and the effects of noise directionality on the acoustic contrast between pixels were examined in a theoretical analysis of a multibeam imaging system [17].

ADONIS consists of a spherical dish faced with neoprene foam, with a diameter of 3 m and a radius of curvature also of 3 m. An array of 130 ceramic *hydrophones* arranged in an elliptical configuration (Fig. 15.2) occupies the focal region of the dish. Each sensor is of square cross section and the center-to-center distance between sensors is 2 cm. The major and minor axes of the array are approximately 0.28 m and 0.22 m, giving an approximate field of view of 6° horizontally and 5° vertically.

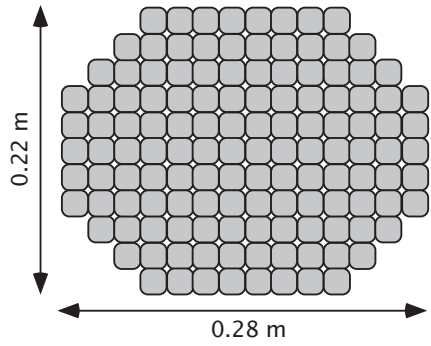

Figure 15.2: *Schematic of the 130-element elliptical array head.*

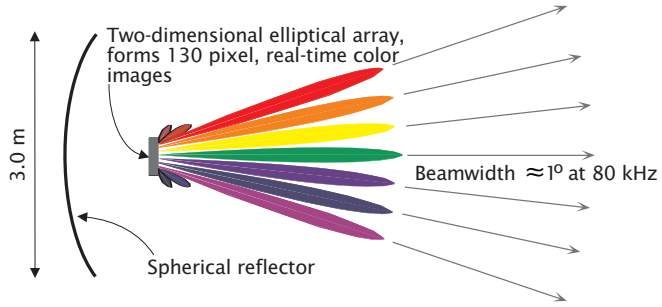

Figure 15.3: *Schematic showing the spherical reflector, array head, and fan of beams; (see also Plate 9).*

A spherical dish was chosen because the aberrations associated with the off-axis receivers are less severe than would be the case with a parabolic reflector. An advantage of the reflector design is that the *beamforming* is performed geometrically, with each hydrophone, by virtue of its position relative to the center of the dish, having its own unique "look" direction. This feature reduces the computational load significantly, as beamforming by the application of phase or time delays to the individual receiver elements is unnecessary. Because the array head contains 130 hydrophones, ADONIS forms a fan of 130 beams (Fig. 15.3) distributed in the horizontal and the vertical. The system operates in the frequency band from 8 to 80 kHz, and at the highest frequency the beamwidth is slightly less than 1°.

To produce the images, the signal in each channel is processed in real time through a custom-built, hybrid analog-digital electronics package. The analog circuitry performs a *spectral analysis* by sweeping a *bandpass filter* with a Q of 4 across the decade of frequency occupied by the signal, and the noise intensity is recorded at sixteen frequency

points uniformly distributed logarithmically through the band. This function is repeated 25 times per second by a switched capacitor filter in each of the 130 channels. The spectral data are then digitized and displayed on a computer monitor as moving, color images, each consisting of 130 pixels. Various signal conditioning options have been developed to improve the quality of the raw images, including interpolation, time-averaging and normalization.

Color in the acoustic daylight images is used in two ways. In most cases, color simply represents the intensity level of the signal in a particular beam, or pixel, averaged over some or all of the sixteen frequency cells. Because the sharpest images are obtained at the highest frequencies, where the beams are narrowest, we have tended to concentrate on the top three frequency cells, covering the band from 58 to 77 kHz.

However, when the lower frequencies are neglected, the broadband capability of ADONIS is not fully exploited. On occasion, the full bandwidth of the system can be used to advantage to yield information about a target, even though spatial resolution may be sacrificed by including lower-frequency data in the image. For instance, the spectral shape of the scattered field from various targets in the object space may differ because of their composition or surface properties, that is to say, they show different acoustic "color." Such targets could, in principle at least, be distinguished from one another through the differences in their scattered spectra. These differences have been visualized in the acoustic daylight images through the second way of using color. By assigning a color to a frequency cell and weighting each color component with the intensity in the cell, the color in the resultant image provides a visual indication of the acoustic and physical properties of the objects in the image. A hollow sphere, for example, may appear as red whereas a solid sphere could be blue. In fact, target recognition through a mapping of the *acoustic color* of an object into visual color in the broadband acoustic daylight image has been demonstrated successfully with certain simple targets of similar shape but different composition.

15.4 Acoustic daylight images

The construction of ADONIS was completed in August 1994. Since then, two major series of acoustic daylight imaging experiments, known as ORB 1 and ORB 2, have been performed with ADONIS mounted on the seabed in San Diego Bay, southern California. In this location, the ambient noise field in the 8 to 80 kHz band is dominated by the sound from colonies of snapping shrimp. These creatures, which are about the size of a thumbnail, generate a random series of disproportionately loud pulses of sound. The duration of each pulse is less than

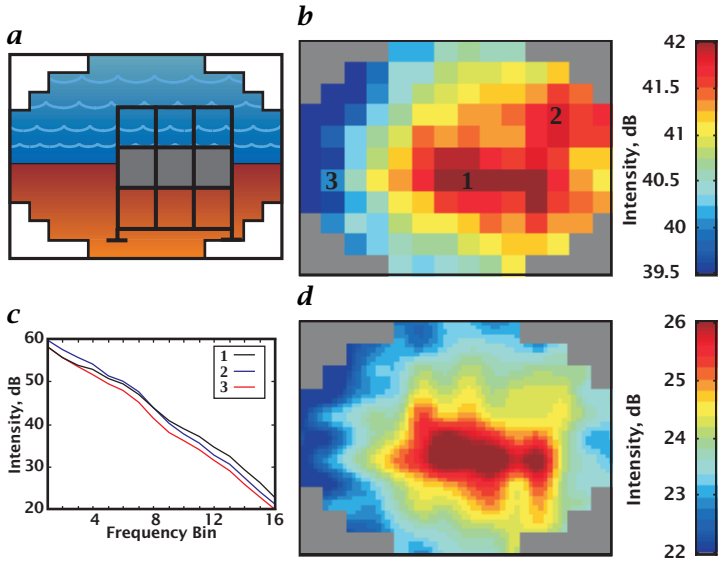

Figure 15.4: ***a*** *Simulated view of the rectangular bar target mounted vertically on the seabed;* ***b*** *acoustic daylight image of the bar target from raw intensity data;* ***c*** *spectra of the pixels labeled 1, 2, and 3 in* ***b****;* ***d*** *interpolated acoustic daylight image of bar target from the same data used in* ***b****. For movies of the same and other targets see* `/movies/15` *on the CD-ROM (*`BarTarget`*,* `BotAirDrum`*,* `BotDrum`*,* `BotSandDrum`*,* `HngDrums`*,* `Sphere`*, and* `Credits`*); (see also Plate 10).*

10 μs and the bandwidth is in excess of 100 kHz. Clearly, such a noise environment is not temporally stationary and in fact gives rise to stability problems in the acoustic daylight images. An effective though not necessarily optimal solution to the difficulty is temporal averaging, which, when performed over about 1 s, corresponding to 25 frames, produces reasonably stable images.

Several different types of targets were used in the ORB experiments, including planar aluminum panels faced with closed-cell neoprene foam, corrugated steel, or a number of other materials. Volumetric targets in the form of 113-liter polyethylene drums, 0.76 m high by 0.5 m diameter, and filled with syntactic foam (essentially air), wet sand or sea-water, have been imaged both in mid-water column and partially buried in the seabed, which consists of a fine-grained silt. A hollow titanium sphere, 70 cm in diameter, has also been imaged in mid-water column. A more mobile target, in the form of a diver with closed breathing system, has been recorded in a series of acoustic daylight images as he swam through the field of view of ADONIS. In most of these imaging experiments, the range between ADONIS and the targets was nominally 40 m.

Figure 15.4 shows two versions of an acoustic daylight image of a horizontal, bar-like target, 1 m high by 3 m wide, and formed from three square aluminum panels faced with neoprene foam. The panels were mounted on a target frame, as illustrated schematically in Fig. 15.4a, and the basic image formed from the raw intensity data is shown in Fig. 15.4b. Each of the square pixels shows the noise intensity in one of the ADONIS beams, averaged over the top three frequency bins (58 – 77 kHz). The noise spectra of the pixels labeled 1, 2, and 3 are shown in Fig. 15.4c, where it can be seen that the background noise level is about 3 dB below the on-target level across the whole frequency band of the system. Figure 15.4d, showing a post-processed version of the same data as in Fig. 15.4b, illustrates the visual improvement over the raw image that can be obtained by interpolation between pixels, in this case by a factor of five.

The acoustic daylight image of the bar target in Fig. 15.4, like many of the images obtained in the ORB experiments, is strongly ensonified from the front. Most of the snapping shrimp sources were located on pier pilings behind ADONIS, which gave rise to a very directional noise field. The strong directionality accounts for the relatively high acoustic contrast between the on-target and off-target regions in the image. Occasionally, a passing vessel ensonified the targets from behind, in which case a silhouette effect was observed in the images. This and other effects appearing in the images are discussed in some detail by Epifanio [18], who also presents acoustic daylight images of all the targets used in the ORB experiments, including the swimming diver.

15.5 Concluding remarks

ADONIS and the ORB experiments have served to demonstrate that ambient noise can be used for incoherent imaging of objects in the ocean. The acoustic contrast achieved in these experiments was typically 3 dB, which is sufficient to produce a recognizable visual realization of the object space. Moreover, ADONIS is unique among underwater acoustic systems in that it produces images continuously in real time at a frame rate of 25 Hz. When shown as a movie, the images show fluid movement and, with appropriate interpolation, averaging and normalization, the objects depicted appear reasonably clearly. Nevertheless, each image contains only 130 pixels and consequently appears rather coarse by optical standards, but it should be borne in mind that ADONIS is a prototype and that more channels could be incorporated into future systems.

Of course, an increase in the number of pixels would represent just one contribution towards improved image quality. Another important factor is the angular resolution that can be achieved, which is governed

by the aperture of the detector measured in wavelengths. In many applications, it would not be practical to extend the physical aperture beyond 3 m, as used in ADONIS. An alternative is to operate at higher frequencies, which may be feasible in areas where snapping shrimp are the main contributors to the noise field, as appears to be the case in most temperate and tropical coastal waters [19, 20]. Signal processing is another means of enhancing image quality. The current acoustic daylight images, such as those in Fig. 15.4, are created by applying simple operations to the noise intensity in each channel. It may be possible to do better, at least in some circumstances, by turning to higher-order statistics; Kalman filtering would appear to have advantages for tracking moving objects [21].

Acknowledgments

Broderick Berkhout generated the spectral data shown in Fig. 15.1 and Chad Epifanio produced the images in Fig. 15.4. John Potter was central to the design and construction of ADONIS. The acoustic daylight research described here is supported by the Office of Naval Research under contract number N00014-93-1-0054.

15.6 References

[1] Urick, R., (1983). *Principles of Underwater Sound*. New York: McGraw-Hill.

[2] Kerman, B., (1988). *Sea Surface Sound: Natural Mechanisms of Surface Generated Noise in the Ocean*. Dordrecht: Kluwer.

[3] Nystuen, J. and Medwin, H., (1995). Underwater sound produced by rainfall: Secondary splashes of aerosols. *J. Acoust. Soc. Am.*, **97**:1606–1613.

[4] Watkins, W. and Schevill, W., (1977). Sperm whale codas. *J. Acoust. Soc. Am.*, **62**:1485–1490.

[5] Watkins, W., Tyack, P., Moore, K. E., and Bird, J. E., (1987). The 20-Hz signals of finback whales (Balaenoptera physalus). *J. Acoust. Soc. Am.*, **82**:1901–1912.

[6] Cato, D., (1991). Songs of humpback whales: the Australian perspective. *Memoirs of the Queensland Museum*, **30**:277–290.

[7] Cato, D., (1992). The biological contribution to the ambient noise in waters near Australia. *Acoustics Australia*, **20**:76–80.

[8] Readhead, M., (1997). Snapping shrimp noise near Gladstone, Queensland. *J. Acoust. Soc. Am.*, **101**:1718–1722.

[9] Cato, D. and Bell, M., (1992). Ultrasonic ambient noise in Australian shallow waters at frequencies up to 200 kHz, DSTO Materials Research Laboratory, Sydney, Report No. MRL-TR-91-23.

[10] Kelly, L., Kewley, D., and Burgess, A., (1985). A biological chorus in deep water northwest of Australia. *J. Acoust. Soc. Am.*, **77**:508–511.

[11] Callen, H. and Welton, T., (1951). Irreversibility and generalized noise. *J. Acoust. Soc. Am.*, **83**:34–40.

[12] Mellen, R., (1952). The thermal-noise limit in the detection of underwater acoustic signals. *J. Acoust. Soc. Am.*, **24**:478–480.

[13] Buckingham, M., Berkhout, B., and Glegg, S., (1992). Imaging the ocean with ambient noise. *Nature*, **356**:327–329.

[14] Buckingham, M. and Potter, J., (1994). Observation, theory and simulation of anisotropy in oceanic ambient noise fields and its relevance to Acoustic Daylight™ imaging. In *Sea Surface Sound '94*, pp. 65–73. Lake Arrowhead, CA: World Scientific.

[15] Buckingham, M., Potter, J., and Epifanio, C., (1996). Seeing underwater with background noise. *Scientific American*, **274**:86–90.

[16] Potter, J., (1994). Acoustic imaging using ambient noise: Some theory and simulation results. *J. Acoust. Soc. Am.*, **95**:21–33.

[17] Buckingham, M., (1993). Theory of acoustic imaging in the ocean with ambient noise. *J. Comp. Acoust.*, **1**:117–140.

[18] Epifanio, C., (1997). *Acoustic Daylight: Passive Acoustic Imaging using Ambient Noise*. PhD thesis, Scripps Institution of Oceanography, University of California, San Diego, CA.

[19] Chitre, M. and Potter, J., (1997). Ambient noise imaging simulation using Gaussian beams. *J. Acoust. Soc. Am.*, **102(5/2)**:3104.

[20] Potter, J. and Chitre, M., (1996). Statistical models for ambient noise imaging in temperate and tropical waters. *J. Acoust. Soc. Am.*, **100(4/2)**:2738–2739.

[21] Potter, J. and Chitre, M., (1996). ADONIS imaging with a Kalman filter and high-order statistics. In *Proc. Third European Conference on Underwater Acoustics*, pp. 349–354, Heraklion: Crete University Press.